Pharmacology Biochemistry & Behavior, Vol. 13, Suppl. 1, pp. 155–165. Printed in the U.S.A.

Lipid-Lipid and Lipid-Protein Interactions in Membranes

PATRICIA C. JOST AND O. HAYES GRIFFITH

Department of Chemistry and the Institute of Molecular Biology
University of Oregon, Eugene, OR 97403

JOST, P. C. AND O. H. GRIFFITH. *Lipid-lipid and lipid-protein interactions in membranes.* PHARMAC. BIOCHEM. BEHAV. 13: Suppl. 1, 155–165, 1980.—Over the past decade spectroscopic methods (fluorescence, ESR, and NMR) have been used to provide new information about the molecular dynamics of lipid-lipid and lipid-protein interactions in membranes. The various methods of characterizing isotropic and anisotropic motion are described. Lipid bilayers are highly dynamic, with rapid acyl chain motion and rapid lateral diffusion in the plane of the membrane. In membranes where proteins penetrate through the bilayer, a large hydrophobic surface area exists in contact with the bilayer lipids. Lipids at the protein interface are in dynamic equilibrium with the remaining pools of bilayer. The protein has been shown spectroscopically to have some influence on the dynamics of the nearest neighbor lipids, leaving the rest of the bilayer relatively unperturbed. Evidence is summarized that, in some cases, the lipid composition in the interfacial region is influenced by the protein.

Lipid-protein interactions Fluorescence techniques Spin labeling Nuclear magnetic resonance
(Na,K)-ATPase Cytochrome oxidase Bacteriorhodopsin Biophysical techniques and membranes

IN the early 1970's Singer [47] proposed a unifying model for the molecular arrangement of lipid and protein in membranes that was based on thermodynamic arguments and the well-known self-association of lipids into bilayers. It pictured much of the protein penetrating into a lipid bilayer matrix. This early model was drawn schematically as shown in Fig. 1, and this model has stood the test of time. In the past decade, the application of a variety of new techniques has provided detailed information about the structure and dynamics of the bilayer. Progress has been made in describing the anisotropic motion occurring in the bilayer, the transbilayer movement of the lipids (flip-flop) and the lateral diffusion and phase segregation of both lipid and proteins. New applications of electron diffraction combined with electron microscopy have provided detailed structural information about two transmembranous membrane proteins, bacteriorhodopsin and cytochrome oxidase. Transmembranous proteins penetrate through the bilayer, creating a hydrophobic lipid-protein interface, and some information is now available about the dynamic behavior of the lipids at this interface. The purpose of this conference paper is to review these new developments.

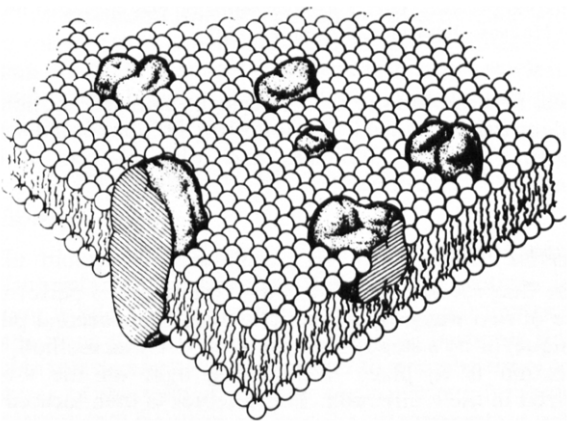

FIG. 1. Schematic drawing of the original fluid mosaic model for membranes, showing globular proteins penetrating into or through the lipid bilayer matrix. Although the proteins are randomly distributed, short range interactions may occur, forming functional oligomers such as the dimer shown here. Reproduced from ref. [48].

A COMPARISON OF SPECTROSCOPIC METHODS OF DETERMINING LIPID DYNAMICS

A number of molecular probes widely used to obtain information about the molecular dynamics of lipids are shown in Fig. 2. Some probes are designed to mimic as closely as possible the structure of naturally occurring lipids while others are not. All probes are designed for use with a specific spectroscopic technique. Fluorescent probes of Fig. 2 include 1,6-diphenylhexatriene (DPH), pyrene (P), 1-anilino-8-sulfonate (ANS), parinaric acid (PnA), a fatty acid anthroyl derivative (AS), and a phospholipid incorporating parinaric acid (PnA-PL). The spin labels of Fig. 2 (fatty acid, phospholipid and steroid spin labels and TEMPO) are monitored by electron spin resonance (ESR) spectroscopy, and the ^{2}H and ^{19}F substituted lipids are designed for observation by nuclear magnetic resonance (NMR) spectroscopy. Useful contributions are being made using each of these techniques.

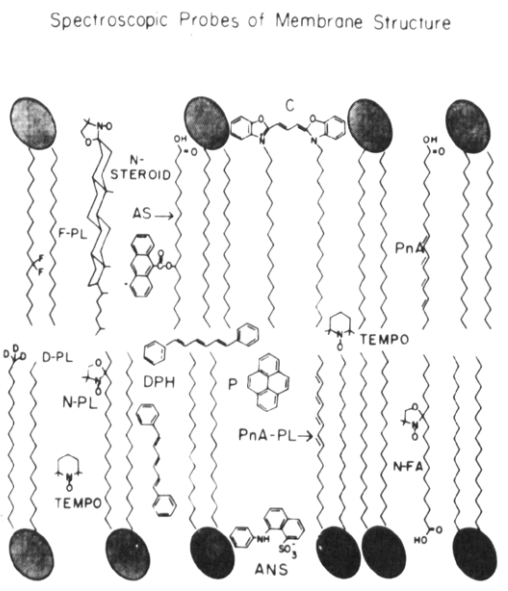

FIG. 2. Schematic drawing of a phospholipid bilayer containing some of the reporter group molecules used in spectroscopic studies of membranes. Fluorescent probes; 12-(9-anthroyl)-stearic acid (AS); a cyanine dye (C); *trans*-parinaric acid (PnA); phospholipid containing *trans*-parinaric acid (PnA-PL); 1,6-diphenyl-1,3,5-hexatriene (DPH); pyrene (P); 1-anilino-8-napthalene sulfonate (ANS). Spin labels (ESR); 3-doxyl-5α-cholestane (N-STEROID); 2,2,6,6-tetramethylpiperidine-1-oxyl (TEMPO); 16-doxylstearic acid (N-FA); phospholipid containing 16-doxylstearic acid (N-PL). NMR labels; selectively fluorinated phospholipid (F-PL); selectively deuterated phospholipid (D-PL). This presentation was suggested by Dr. Bruce Hudson. Reproduced from ref. [30].

We will first discuss the simpler case of isotropic motion to introduce the techniques. The following sections will discuss anisotropic motion, diffusion, and other aspects of the dynamics of membranes.

Isotropic Motion

The fluorescence spectroscopy experiment is performed in one of two ways: by a kinetic method (nanosecond pulse technique) or by a steady state method. In either method, the convention is to place the exciting light on the x-axis polarized in the z direction. The detector is then located on the y axis and the quantities measured are the fluorescence intensities with the analyzer parallel ($I_\parallel$) and perpendicular ($I_\perp$) to z, respectively. The normalized difference between these two experimental quantities is reported as either the emission anisotropy (r) or the polarization (P) where $r=(I_\parallel-I_\perp)/(I_\parallel+2I_\perp)$ and $P=(I_\parallel-I_\perp)/(I_\parallel+I_\perp)$. The relationship between these two quantities is $(1/P-1/3)=2/3r$. In the absence of motion, $r=2/5$ and $P=1/2$. (These values assume that the absorption and emission transition dipoles are parallel. This is the case for *trans*-parinaric acid and 1,6-diphenylhexatriene. The transition dipoles are approximately parallel to the long molecular axes of these asymmetric molecules. For the case of an arbitrary angle between the two transition dipoles see ref. [4], p. 461. In this reference and approximately half the literature, the symbol A is used for emission anisotropy instead of r.) As the fluorescent molecules undergo molecular motion, depolarization occurs; r and P decrease and finally become zero for sufficiently rapid isotropic tumbling (i.e., $I_\parallel=I_\perp$).

In the kinetic method, the two decay curves $I_\parallel(t)$ and $I_\perp(t)$ are measured separately and the emission anisotropy takes the time-dependent form

$$r(t)=[I_\parallel(t) - I_\perp(t)]/[I_\parallel(t) + 2I_\perp(t)] \qquad (1)$$

Defined in this way, the emission anisotropy is a ratio of decay curves that factors out the fluorescence lifetime and depends only on the rotational motion of the fluorescence probe. For a rigid spherical molecule undergoing isotropic tumbling, the decay is described by a single exponential

$$r(t)=r_0\, e^{-t/\tau_c} \qquad (2)$$

where τ_c is the correlation time. This kinetic method of obtaining τ_c is gaining in popularity since the introduction of commercial pulsed spectrometers and suitable laser sources. The advantage is that the measurement is direct and any significant deviation from a single exponential decay curve can be readily seen.

The static method of obtaining τ_c historically has been the most widely used. In this method, the experimental quantities are time averages of $I_\parallel(t)$ and $I_\perp(t)$, designated $\bar{I}_\parallel$ and $\bar{I}_\perp$. The interpretation of these experiments is based on the Perrin equation, the integrated form of the single exponential fluorescence decay case. In terms of the static emission anisotropy, r, the Perrin equation takes the form

$$\frac{r_0}{\bar{r}} = \left(1 + \frac{\tau_f}{\tau_c}\right) \qquad (3)$$

In terms of the static polarization $\bar{P}$, the Perrin equation takes the slightly more complicated form

$$\left(\frac{1}{\bar{P}} - \frac{1}{3}\right) = \left(\frac{1}{P_0} - \frac{1}{3}\right)\left(1 + \frac{\tau_f}{\tau_c}\right) \qquad (4)$$

In these expressions r_0 and P_0 are the static anisotropy and polarization observed in the absence of motion and τ_f is the fluorescence lifetime. To apply the Perrin equation, a hydrodynamic model of a sphere tumbling in an isotropic medium is usually assumed. The appropriate form of the Stokes-Einstein equation is $\tau_c=\eta V/kT$ where η is the viscosity, V is the molecular volume, k is the Boltzmann constant, and T is the absolute temperature [4,51]. The static $\bar{I}_\parallel$ and $\bar{I}_\perp$ are measured as a function of T/η. When $(\bar{r})^{-1}$ or $(1/\bar{P} - 1/3)$ is plotted versus T/η, a straight line should result. Assuming τ_f is known, the slope gives the molecular volume V and the intercept determines r_0 or P_0. With these quantities, τ_c can be calculated from the above Perrin equation at the desired viscosity and temperature. This method of estimating τ_c has the advantage of requiring simpler equipment but suffers from several disadvantages. The fluorescence life-time must be measured separately or assumed to be constant over the range of temperatures and viscosities studied. τ_c can be calculated only if r_0 (or P_0) is known, but this quantity must be determined indirectly or taken from literature values. Without the decay curves it is difficult to establish that only a single exponential decay curve is involved. In spite of these problems, the Perrin equation has been shown to yield values of τ_c comparable to the more direct kinetic method for an isotropically tumbling fluorescent labeled protein [20]. The anisotropic motion that is seen in membranes is more troublesome and is discussed later.

In fluorescence spectroscopy, information is obtained regarding molecular motion when the rotational motions are on the order of the fluroescence lifetime (typically nanoseconds). The directions of the absorption and emission transi-

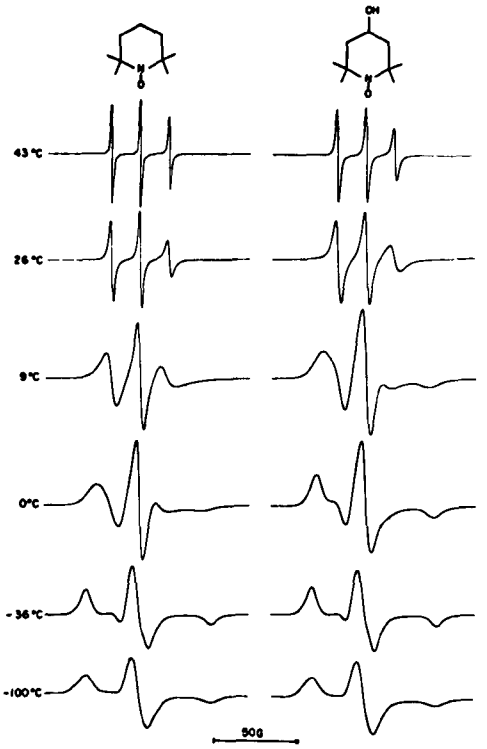

FIG. 3. The effect of viscosity on the ESR spectrum of two small nitroxides tumbling in glycerol. The spin label concentration was 5×10^{-4} M, and the samples were sealed in quartz tubes to exclude water vapor. Note the characteristic line broadening and overlap seen as the temperature is lowered. The tumbling is essentially isotropic, but differences in hydrogen bonding with the glycerol probably account for the lineshape differences seen when the two labels are at the same temperature. At temperatures higher than 43°C, both spectra will reach the limits of three lines of equal intensity. Reproduced from ref. [28].

tion dipoles are fixed in the molecule. If the molecule rotates through a significant arc in the time interval between absorption and emission, depolarization occurs (i.e., $I_{\parallel}$ and $I_{\perp}$ begin to converge). This depolarization provides a method of estimating τ_c as described above.

The spin labeling experiment (ESR) also involves a consideration of dipoles, but of a fundamentally different nature. The spin label is a stable free radical in which the stable N-O group has the unpaired electron. This unpaired spin senses the combined magnetic fields of the laboratory magnet and the smaller perturbing field of the nearby ^{14}N nucleus. The nuclear spin of ^{14}N is 1, consequently there are three orientations in the magnetic field (+1, 0, −1) resulting in three absorption lines in the ESR spectrum, with the individual lines separated by the coupling constant A. There are two components in the magnetic interaction. One arises because of the small but finite probability of finding the electron at the ^{14}N nucleus (called the Fermi contact interaction), and this term is isotropic. Consequently, there is always a finite value of A even when the spin label is tumbling rapidly in solution. In addition there is a magnetic dipolar interaction between the ^{14}N nuclear spin and the unpaired electron. This interaction is modulated by molecular motion causing line shape changes as shown in Fig. 3, where the sample temperature is varied. From these line shapes, the molecular motion of the spin label can be inferred. For isotropic tumbling, this can be described by a single correlation time, τ_c. Except for tumbling ranges rapid enough to maintain clear separation of the three lines, values of τ_c are obtained by comparing experimental spectra with computer-generated theoretical line shapes [13]. In the limit of very fast tumbling (e.g., $\tau_c \sim 10^{-11}$ sec) the dipolar interactions are essentially completely averaged out, leaving a sharp 3-line spectrum.

Deuterium NMR is a more recent entry into the field of molecular probe techniques. The deuterium nucleus experiences two interactions, one with the external magnetic field and the other arising from an electrostatic interaction of the deuterium quadrupole moment with the electric field gradient at the nucleus. This quadrupolar term is anisotropic and averages to zero in a rapidly tumbling molecule (e.g., $\sim 10^{-6}$ sec) leaving only a single line NMR spectrum at the fast motion limit. When the molecular motion is slower than this, the quadrupolar interaction is modulated by molecular motion and information can be obtained from the analysis of line shapes and relaxation times [42,43].

In the isotropic tumbling case, which is the only case we have discussed so far, the spectra can be characterized in terms of a single parameter. There are three current conventions, the rotational correlation time, the rotational relaxation time, and the rotational diffusion constant. The rotational correlation time (τ_c) is the time required for the average value of the function $(1/2)(3\cos^2\theta_t - 1)$ to change from 1 to 1/e, i.e., $(1/2)\langle 3\cos^2\theta_t - 1\rangle = e^{-t/\tau_c}$. This expression is common to NMR, ESR, and fluorescence spectroscopy. The rotational relaxation time (ρ or ϕ) is the time required for the average value of $\cos\theta_t$ to change from 1 to 1/e, i.e., $\langle\cos\theta_t\rangle = e^{-t/\rho}$. This functional relationship is used in dielectric relaxation studies and sometimes in fluorescence studies. The rotational diffusion constant, D_r, is the usual constant appearing in the classical rotational diffusion equation. The relationships between these three quantities are $\rho = 3\tau_c$, $\tau_c = 1/6D_r$, and $\rho = 1/2D_r$ [5].

DYNAMICS IN LIPID BILAYERS AND MEMBRANES

Anisotropic Motion

In biological membranes, the lipid bilayer solvent is antisotropic. A rigorous description of the motions in the bilayer would require the time-dependent coordinates of all atoms along the lipid chain. For practical purposes it is desirable to use only a few parameters to describe the essential features of the motion. Clearly the equations for isotropic motion cannot be used to describe bilayer motion without some modifications. The phospholipid molecule is not free to tumble isotropically, thus the motions of the lipid chains or probes are restricted.

A special case, but one that is used widely in the membrane field, assumes axially symmetric motion about a symmetry axis. One measure of the fluctuation of molecular axes is the order parameter, S, which is defined as

$$S = (1/2)\langle 3\cos^2\theta - 1\rangle \qquad (5)$$

where θ is the angle between the fluctuating molecular axis and the reference axis (the director). The director axis is usually taken to be normal to the plane of the bilayer surface. S varies in value between 0 and 1 when the unique reporter group axis is parallel to the long molecular axis. S=0 corresponds to complete averaging over all angles, and S=1 corresponds to the absence of motion of the long axis (except

for spinning of the long axis). This order parameter equation assumes axial symmetry and rapid motion over a characteristic time, t, which is dependent on the technique. Thus, the order parameter provides a measure of the amplitude of motions that occur with frequencies larger than $1/\pi t$. The order parameter is a time-averaged quantity, and it does not imply macroscopic alignment in the system. For example, a randomly oriented collection of molecules in a frozen sample would still correspond to the limiting case of S=1. Order parameters can be related to experimentally obtained quantities from fluorescence, ESR, and NMR.

In the kinetic (pulsed) fluorescence experiment

$$S^2 = \frac{r_\infty}{r_o} \qquad (6)$$

where r_∞ is the final limiting value and r_o is the initial value of the emission anisotropy [21]. This equation applies to molecules such as *trans*-parinaric acid and DPH where the parallel absorption and emission transition dipole moments coincide with the long molecular axis. In principle, the time-domain fluorescence experiment provides a method for distinguishing between isotropic tumbling and anisotropic motion of limited amplitude. For the isotropic case, the decay curve is a simple exponential decay described by Equation 2, whereas in the restricted amplitude case, the fluorescence anisotropy decays roughly according to the relationship

$$r_t = r_\infty + (r_o - r_\infty)e^{-t/\tau_c} \qquad (7)$$

The two parameters S and τ_c are derived from this experiment, and an example is given in Fig. 4. The three fluorescence anisotropy decay curves are for *trans*-parinaric acid in liposomes of the saturated phospholipid, dipalmitoyl phosphatidylcholine, with increasing concentrations of cholesterol. All three curves show a plateau region that provides information for the order parameter. The initial decay of all three curves is essentially the same. The interpretation is that the presence of cholesterol has little effect on the rotational correlation time of the molecular probe, but decreases the amplitude of the motion in the phospholipid bilayer. Similar experiments have been reported with DPH [33,55].

The static fluorescent analog to Equation 7 is a modified Perrin equation.

$$\frac{r_o - r_\infty}{\bar{r} - r_\infty} = \left(1 + \frac{\tau_f}{\tau_c}\right) \qquad (8)$$

However, it is difficult to measure separately r_∞ and τ_c in this experiment. Several authors have taken the approach of using the isotropic Perrin equation (Equations 3 or 4) and the Stokes-Einstein equation with a shape parameter to describe the fluorescence depolarization of a non-spherical probe (e.g., ref. [46]). Changes in membrane properties can produce changes in τ_c and S, and this approach interprets all effects as changes in τ_c. Since the calculated microviscosity is formally linked to changes in τ_c and not S, this procedure can lead to overestimates of changes in microviscosity. Nevertheless, it is useful to use the static fluorescence experiment to sense a change, which can then be explored further with the pulsed fluorescence technique.

In spin labeling, the order parameter is given by

$$S = \frac{\bar{A}_\parallel - \bar{A}_\perp}{A_{zz} - (1/2)(A_{xx} + A_{yy})} \cdot \frac{a}{a'} \qquad (9)$$

where $a=(1/3)(A_{xx} + A_{yy} + A_{zz})$ and $a'=(1/3)(A_\parallel + 2A_\perp)$. The quantities $\bar{A}_\parallel$ and $\bar{A}_\perp$ are measured from the ESR spectrum, A_{xx}, A_{yy} and A_{zz} are anisotropy parameters obtained from single crystal data, and a/a′ is a polarity correction. This equation is appropriate for the widely used doxyl and proxyl fatty acids and phospholipids, where the large splitting occurs with the magnetic field parallel to the long molecular axis [17,18].

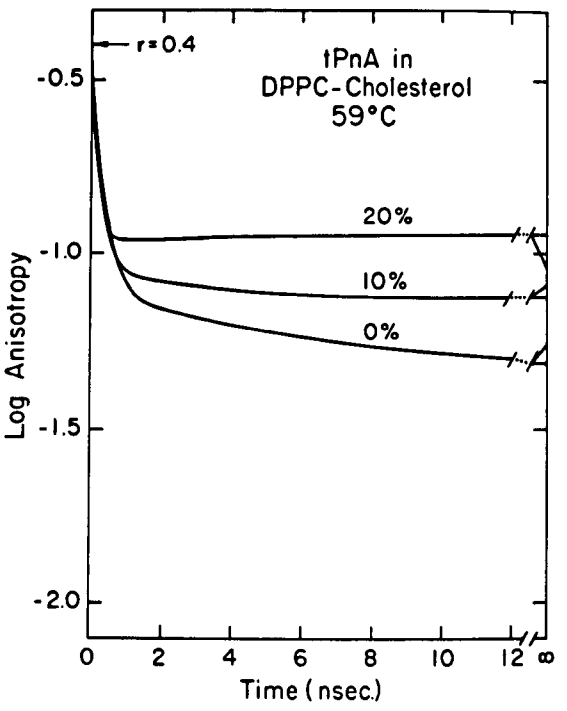

FIG. 4. The decay of the fluorescence polarization anisotropy of *trans*-parinaric acid in DPPC/cholesterol bilayers at 59°C. The samples are multilamellar liposomes at a total lipid concentration of 0.15 mM in 100 mM phosphate buffer at pH 7.2 and labeled with one *trans*-parinaric acid per 100 lipids. The fluorescence excitation source was ultra-violet radiation from the storage ring at the Stanford Synchrotron Radiation Laboratory. The time resolution of the electronics is about 700 psec. The horizontal extrapolation to "infinity" refers to the evaluation of the fit r(t) curve, i.e., the value is the constant term in this fit. The diagonal line at the right refers to a direct reading of r(t) at a "long" time without deconvolution for the excitation pulse or any assumption of a functional form for r(t). The difference between these two values may be considered as an estimate of the uncertainty in r(t) at long times. (P. K. Wolber and B. Hudson, personal communication.)

Deuterium NMR also provides an order parameter. In ^2H NMR of a randomly oriented sample of bilayers, the splitting between the two peaks ($\Delta\nu_Q$) is related to an order parameter S_{CD} by the equation

$$\Delta\nu_Q = \frac{3}{4}\frac{e^2qQ}{h}S_{CD} \qquad (10)$$

where (e^2qQ/h) is the static quadrupolar coupling constant, about 170 kHz in aliphatic C-D bonds. S_{CD} represents a time average value over any fluctuations of the C-D bond that are rapid compared with 170 kHz. The C-D bond is not in general parallel to the long molecular axis of the lipid chain; consequently, a further transformation is required to obtain an order parameter, often called S_{mol}, comparable to those derived from other techniques. S_{mol}, but not S_{CD}, has the limits of S=1 (no motion) and S=0 (complete averaging) [43].

Data from Raman spectroscopy have also been used to define an order parameter [16]. This method is based on the

observation that a portion of the Raman spectra of phospholipids is sensitive to the conformational state of the hydrocarbon chains. For example,

$$S_{trans} = \frac{(I_{1133}/I_{ref})_{observed}}{(I_{1133}/I_{ref})_{standard}} \qquad (11)$$

where I_{1133} is the intensity of a Raman band at 1133 cm^{-1} and I_{ref} (observed) is the intensity of the choline head group C-N stretch at 722 cm^{-1}. The corresponding quantities in the denominator are for a solid sample of dipalmitoyl lecithin which is in the all *trans* configuration. Thus, $S_{trans}=1$ when the lipid is in the all *trans* configuration, and S_{trans} decreases with increasing proportions of *gauche* forms. This expression has not been derived in terms of the order parameter formalism, but can be a useful empirical quantity.

In general, the order parameter, S, is a measure of the probability distribution (amplitude) of angles sampled by the reporter group in a time that is short compared to the time scale of the technique used. A simplified picture is the cone model (Fig. 5) where the long molecular axis executes a restricted random walk about the director axis, and this motion is confined to a cone of half-angle γ [27]. The relationship between γ and the order parameter is

$$S=1/2\ (\cos\gamma + \cos^2\gamma) \qquad (12)$$

This description of anisotropic motion provides a measure of the amplitude, S, and at least a lower limit to the frequency (τ_c^{-1}).

Flexibility Profile

It has been observed by ESR and NMR that the motion of the lipid chains (*gauche-trans* isomerizations) increases toward the center of the bilayer. In magnetic resonance, the order parameter provides a measure of the amplitude and the lineshapes give information about the frequency of motion. The order parameter is largest near the polar head group and smallest at the hydrocarbon terminus [25, 27, 38, 44]. An example is shown in Fig. 6 where the values of S are given for phospholipid bilayers in the presence and absence of cholesterol. From left to right, the nitroxide moiety is attached at positions progressively farther from the carboxyl end of the chain. The presence of cholesterol decreases the amplitude of motion, which is often referred to as the "ordering" effect of cholesterol. The same general trend is observed by ^{2}H-NMR although details of the shape are different [44]. These differences may be due both to the perturbation of the spin label and to the differences in the time scale of the two techniques. Results from both techniques are consistent with the picture that the amplitude and frequency of segmental motion of bilayer lipid chains increases dramatically toward the center of the bilayer.

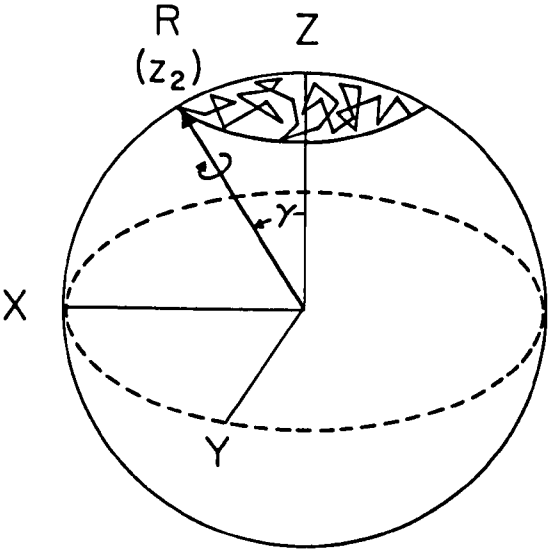

FIG. 5. The cone model for restricted motion. Within the cone, molecular motion is fully allowed. The arrow, corresponding to the nitroxide z axis, executes a rapid random walk, pointing with equal probability in all directions with the cone defined by the angle γ, which is the angle between the z axis (director axis) and the direction normal to the bilayer plane [27].

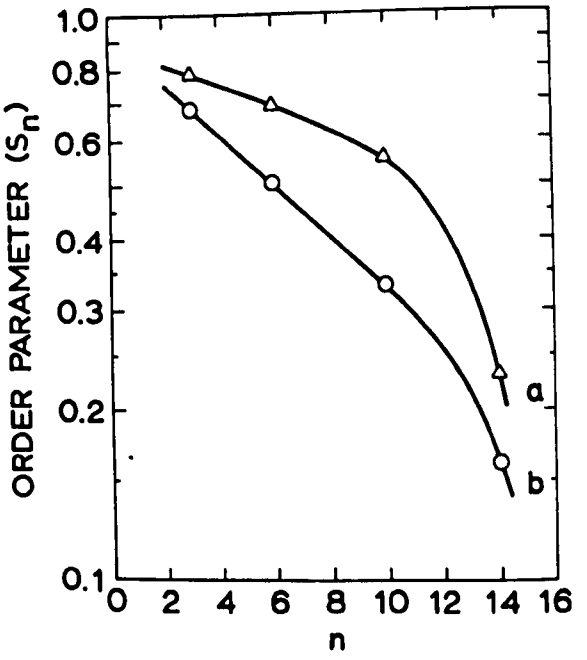

FIG. 6. The order parameter as a function of n, where n+2 gives the number of carbons counting from the carboxyl end of the fatty acid chain. The samples are fully hydrated multilayers of (a) egg lecithin with cholesterol, 2:1 and (b) egg lecithin without cholesterol. Reproduced from ref. [39].

Lateral and Rotational Diffusion in Membranes

Mobility of proteins in membranes was first demonstrated in the early 1970s [7, 14, 50]. Since then the lateral diffusion coefficients of many lipids and proteins have been reported, as well as changes in the mobility and aggregation of cell surface components and control of these processes.

Lateral diffusion of lipids in the plane of the membrane has been measured using spin labeled lipids, fluorescent phospholipids probes, and NMR probes. The ESR technique relies on magnetic interactions between spin-labeled lipids, which decrease with diffusion (i.e., dilution) in the kinetic experiment [9], or affect the lineshape in the equilibrium experiment [53]. The fluorescence measurements are obtained in three related ways. All of them follow the lateral movement of the probes with a fluorescence microscope. The fluorescence photobleaching recovery [1] and periodic pattern photobleaching [49] methods involve transient responses after a disturbance. The third method, fluorescence

correlation spectroscopy [36], measures fluctuations about an equilibrium. Useful reviews of translational diffusion include [6, 10, 11]. The various techniques rely on very different kinds of measurements, each with its own set of limitations, possible artifacts and advantages. The remarkable result is that there is general agreement on the rates of lateral diffusion of phospholipids. Typical diffusion rates in liquid crystalline bilayers are on the order of 10^{-7} to 10^{-8} cm^2 sec^{-1}. Thus, lateral diffusion is quite rapid. To get a better idea of just how rapid, it is useful to calculate the distance traveled assuming no obstructions. The time t required to travel a distance Δx is determined from the equation $(\Delta x)^2=4Dt$. In this simple model, which ignores boundary conditions, the amount of time it would take for a phospholipid to diffuse from one end of a 10 μ long cell to the other end is $t=\Delta x^2/4D \approx (10^{-3}\ cm)^2/4(2\times10^{-8}\ cm^2\ sec^{-1})=12$ sec. Another way to get a feeling for the magnitude of the diffusion constant is to equate diffusion to a random walk model. For example, a diffusion constant of 10^{-8} cm^2 sec^{-1} corresponds to a hopping frequency between adjacent sites in the bilayer of about $10^6 - 10^7$ sec^{-1} [53]. The translational diffusion rates, of course, decrease at lower temperatures.

Translational diffusion rates of proteins are much smaller due to the increased size of the particles. Typical values range from $2\text{–}6\times10^{-9}$ cm^2 sec^{-1} for rhodopsin to $1\text{–}3\times10^{-11}$ cm^2 sec^{-1} for several lectin receptors, surface antigens, and acetylcholine receptors [6]. Diffusion constants for larger oligomeric associations such as may occur in gap junctions or among proteins in the mitochondrial respiratory chain could be very much smaller. These very slow diffusions become difficult to measure because of convection or rotational motion of the whole vesicle or membrane.

Rotational motion of proteins is measured by fluorescence or phosphorescence spectroscopy and by saturation transfer ESR spectroscopy. The usual assumption is to replace the single diffusion constant D_r for isotropic motion ($D_r=1/6\ \tau_c$) by two diffusion constants $D_\parallel$ and $D_\perp$. The important parameter is $D_\parallel$, which describes rotation about an axis normal to the plane of the membrane. Membrane proteins are amphipathic and for thermodynamic reasons cannot undergo reorientation about axes parallel to the plane of the membrane, so that $D_\perp \approx 0$. The emission anisotropy in the pulsed fluorescence or phosphorescence experiment then takes the form [6]

$$r_{(t)}=\left[\frac{r_0}{A_1+A_2+A_3}\right][A_1 \exp(-D_\parallel t) + A_2 \exp(-4D_\parallel t) + A_3] \quad (13)$$

where A_1, A_2, and A_3 are angular factors that depend on the orientation of the transition dipole moments relative to the bilayer normal. Rotational diffusion is a special case of anisotropic motion and so Equation 13 bears a relation to Equation 7. (In the order parameter formalism, rotation is equivalent to $S=1$ with continued reorientation about the director axis.) The diffusion coefficient $D_\parallel$ is then linked to viscosity through a form of the Stokes-Einstein equation appropriate for a smooth cylinder in a continuous fluid. There are difficulties with applying hydrodynamics to two-dimensional fluids, but the numbers can be regarded as useful relative estimates. The measurable time scales are set by the emission lifetime of the probe and typically range from 10^{-8} to 10^{-9} sec for fluorescence and $>10^{-3}$ sec for phosphorescence. The saturation transfer ESR spectroscopic method [26] is also sensitive to a wide range of rotational correlation times (10^{-7} to 10^{-3} sec). Among the problems of applying these techniques are the following: determining the principal direction of the probe with respect to the normal to the bilayer; selective labeling of the proteins; and possible motion of the probe itself independent of the motion of the protein.

Rotational motions of proteins are often reported as rotational relaxation times ($\phi_\parallel=1/D_\parallel$). Typical values of $\phi_\parallel$ for membrane proteins lie in the range from 10^{-4} to 10^{-5} seconds.

There is some controversy arising from the various measures of anisotropic motion in membranes. This is to be expected. As an analogy, consider a parable about four people recording the behavior of a wheat field on a windy day. One person photographs the undulating waves of wheat with a camera using a slow shutter speed (ESR or fluorescence spectroscopy). From the blurred image this photographer estimates an amplitude of motion (order parameter), and from the shutter speed of the camera, assumes a lower limit for the time required for movement through a significant arc (rotational correlation time). The second photographer uses an even slower shutter speed (NMR) and reports larger amplitude motion (lower order parameters). These two photographers might disagree as to the frequency of motion (τ_c^{-1}), but they would agree that the amplitude of the movement of the heads of the grain is large compared to that of the base of the stalk (flexibility gradient) and is dependent on the wind speed and turbulence (temperature). A third observer chooses to record how foreign objects (e.g., DPH or pyrene) tumble in the field. More rapid motion or larger amplitude oscillations are taken as a measure of increased fluidity. The fourth observer bleaches a small patch of the field (fluorescence photobleaching recovery) and observes that no normal wheat stalks migrate into the bleached area, and concludes that there is no fluidity at all ($D_\parallel=0$). Here is where the analogy breaks down, since in bilayers the lipid polar groups are "rooted" at the aqueous interface, but may exchange laterally with other lipids to produce a rapid diffusion. Nevertheless, the parable makes a point. The same four observers would have no difficulty agreeing on the difference in rotational motion of a smooth spherical object tumbling in water and molasses, but it will take some time for them to reconcile the differences in interpretation of measurements in anisotropic systems.

Transbilayer Movement of Lipids (Flip-Flop)

From the variety of motions now known to be present in membranes, it is clear that there may be various time-dependent changes in the composition of regions in the plane of the membrane. The membrane is also compositionally different from one side of the bilayer to the other, i.e., in all membranes the lipids in the external half of the bilayer tend to be different from those on the cytoplasmic side. From the accumulated evidence over the past few years, the neutral phospholipids (phosphatidylcholine and sphingomyelin) and the glycolipids predominate in the external leaflet and negatively charged lipids predominate in the leaflet on the cytoplasmic side [41,52], with membrane proteins vectorially inserted.

The origin and maintenance of the compositional asymmetry of the bilayer is a problem of current interest. The maintenance of the transbilayer lipid asymmetry suggests that exchange of phospholipids across the bilayer must be slow relative to the other dynamics involved. The best estimate available from a variety of techniques is that spontaneous transbilayer exchange of lipids (flip-flop) is very slow, on

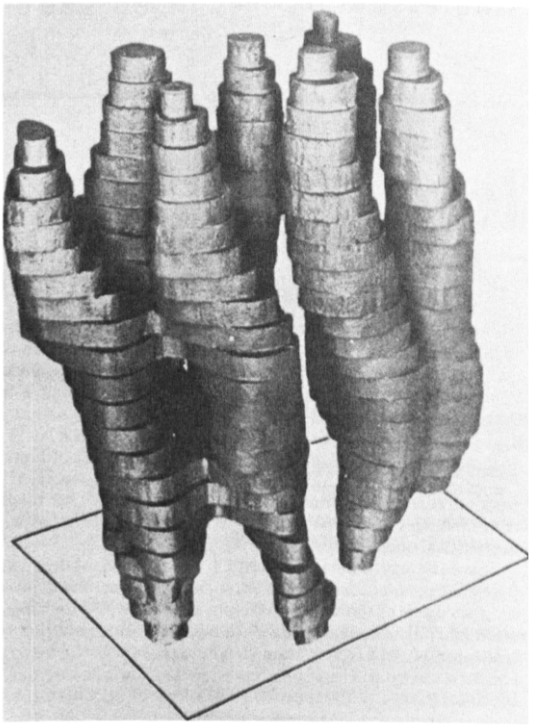

FIG. 7. A model of the bacteriorhodopsin molecule showing the seven individual helices of the polypeptide as they span the membrane. The top and bottom correspond to the regions in contact with the aqueous interface, the rest being in contact with the lipid. Reproduced from ref. [22].

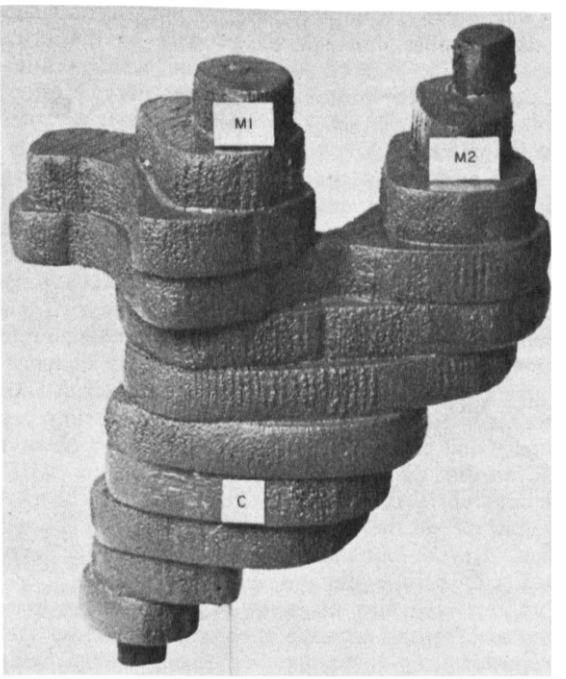

FIG. 8. Model of the general shape of the cytochrome *c* oxidase monomer. M1 and M2 extend into the matrix but are thought to be largely surrounded by lipid, while the C domain extends well beyond the bilayer. The molecule is roughly 100 Å long and is presented at a resolution of 25 Å. The seven helices in bacteriorhodopsin, shown in Fig. 7, would fit approximately into one of the two arms of the Y-shape. Reproduced from ref. [15].

the order of days or even months. On the other hand, enzyme facilitated movement, accompanied by changes in head group composition is relatively fast [23,24] and may play a role both in the origin of lipid asymmetry and in various cellular functions.

THE DYNAMICS OF LIPID-PROTEIN INTERACTIONS

In the Singer model, the proteins are globular and many penetrate through the lipid bilayer. It has been difficult to get information about the structure of these proteins, because they combine with lipids or detergents to give, at best, small patches of two-dimensional crystals, and three-dimensional crystals suitable for x-ray diffraction have been difficult to obtain. Unwin and Henderson [54] have developed a new method of obtaining details of three-dimensional structure from small two-dimensional crystalline arrays by combining intensity information from electron diffraction with phase information from electron micrographs. The shapes of two transmembranous proteins have been determined by this method. Figure 7 shows the model of bacteriorhodopsin, a specialized protein occurring in patches in *Halobacterium halobium*. The seven helical segments of the 26,000 molecular weight polypeptide span the membrane, and are about 40 Å long and 10 Å apart [12]. Cytochrome oxidase, the terminal member of the mitochondrial respiratory chain, carries out the transfer of electrons from cytochrome *c* to molecular oxygen. This is a much larger multipeptide protein (140,000–200,000 molecular weight). The reconstruction of the general shape of this molecule is shown in Fig. 8. It has three domains, M1, M2, and C. The molecule spans the membrane. M1 and M2 are roughly 50 Å in length, are separated by 40 Å, and are on the matrix side of the membrane largely buried in the lipid. The C domain (roughly 55 Å long) is exposed on the other side of the bilayer. At this resolution individual helices are not resolved for cytochrome oxidase, but the molecular shape is a distorted Y structure and the tail of the Y extends well beyond the bilayer [15].

Since these and many other membrane proteins span the bilayer, lipids surround and directly contact the protein surfaces. There has not been general appreciation of the substantial fraction of the lipid that is involved at this lipid-protein interface. In native membranes such as the retinal rod outer segment discs and the sarcoplasmic reticulum, where a single protein of known molecular weight predominates, it is possible to calculate (from the compositional data and approximate protein geometry) that 25–45% of the lipid must be in instantaneous contact with the hydrophobic protein surfaces. Nature has been very efficient in packaging functional proteins in membranes, and the model of Fig. 1 should be redrawn to show a much higher density of protein. These boundary regions are important, because it is here that the lipids of the bilayer are most likely to affect functions of the protein.

The relatively short time scale of ESR has made it possible to detect lipid spin labels contacting hydrophobic surfaces of the protein [2, 3, 29, 35, 56]. In general, when protein is in the bilayer, two spectral components are present corresponding to the equilibrium concentrations of lipid spin labels at the protein boundary and in the bilayer. By varying the lipid to protein ratio, it has been shown in several sys-

tems that there is a large number of lipid contact sites and that the number corresponds roughly to the calculated perimeter of the protein. At physiological temperatures the lipid contacting the protein exhibits restricted motion compared to the fluid bilayer. This, however, does *not* mean that these lipids bind tightly to the protein. The available spectroscopic evidence suggests that most of these interfacial lipids have a very low energy of interaction with the protein, and that the restricted motion results from the lipid conforming to the irregular protein surface. ESR experiments have demonstrated that lipid in the boundary region is exchanging with bilayer lipid [31]. A wide range of exchange rates would be compatible with the ESR data, since exchange rates approaching the rate of lateral diffusion in the bilayer would still give rise to two spectral components. Recent NMR experiments have confirmed the dynamic equilibrium between boundary and bilayer. Only one component is observed by NMR, so that the exchange rate is fast on the NMR time scale but slow on the ESR scale [8, 40, 45]. This brackets the exchange rate of the bulk of the lipid between about 10^3 to 10^7 sec^{-1} for the limited number of systems that have been looked at by both techniques.

The time-scale and sensitivity of the line shape to motion have made the spin-labeling experiment the most useful of the reporter group techniques for distinguishing the lipid in contact with the protein. However, spin labeling experiments on membranes, native and reconstituted, require considerable care in the analysis of digitized data. The problem is illustrated in Fig. 9, where pairs of spectra are summed to give equal concentrations of spin labels from both components in the final summed line shape. The top spectrum in each pair on the left is the bilayer line shape and the one below is the protein-associated line shape. Note that in the summed spectrum, the narrow bilayer lines tend to dominate even though the protein-associated component represents 50% of the intensity. This effect leads to the visual impression that there is little motion-restricted component present. Furthermore, as the temperature is increased (primarily reflected in further narrowing of the fluid bilayer spectrum) the motion-restricted broad component appears to melt away, leaving only the prominent bilayer line shape. In this case, the relative contributions to the final line shape are known.

When the spin label moiety is nearer the hydrocarbon terminus than in this example (i.e., at the C_{16} position rather than the C_{14} position of the C_{18} acyl chain), the effect seen in Fig. 9 is exaggerated. The broad line shape is unchanged, but at comparable temperatures the bilayer lines are even narrower than those shown here. On the other hand, at very low temperatures the bilayer spectrum becomes very broad and can give the impression that the bilayer has disappeared. At temperatures low enough to approach the transition temperature of the lipids, the assumptions of the analytic technique break down, and meaningful spectral analysis at these temperatures is not possible in most cases.

In the membrane experiment, the experimental composite line shape is analyzed into the individual spectral components by one of the several methods [3,32]. It is not surprising that in some cases misinterpretation and controversy have resulted.

It is of considerable interest to determine the equilibrium distribution of lipids in contact with the hydrophobic surface of the membrane protein. The ESR line shape indicates only that the bulk of the lipid spin labels in contact with the protein exhibit motion that is quite restricted compared to

FIG. 9. The effect of line shape changes in individual components on the final composite ESR spectrum. Left column: The pairs of spectra are scaled arbitrarily to the same center line height. The upper spectrum of each pair is characteristic of the 14-proxylphosphatidylcholine in lipid bilayers. The bottom spectrum of each pair shows the line shapes of the broad protein-associated components. The changes in these individual line shapes, from top to bottom, are characteristically seen with increasing temperature, as the bilayer lines narrow and the outermost features of the broad component decrease slightly. Right column: The summed spectra were obtained by integrating and summing, so that two components on the left are present in equal amounts. The change in line shape from top to bottom mimics the line shape changes that occur with increasing temperature. Note that both components remain present in the same ratio, despite the radical changes in appearance.

the motion of fluid bilayers. Although line shapes provide no information regarding the binding constants of the spin label relative to the unlabeled lipid, the integrated intensities can be used to obtain this information. The equilibrium can be formulated as an exchange reaction between a lipid of one class (L*) and the reference solvent lipid (L) occupying n binding sites on the surface of the protein, P [19]:

$$L^* + L_nP \rightleftarrows L + L^*L_{n-1}P \qquad (14)$$

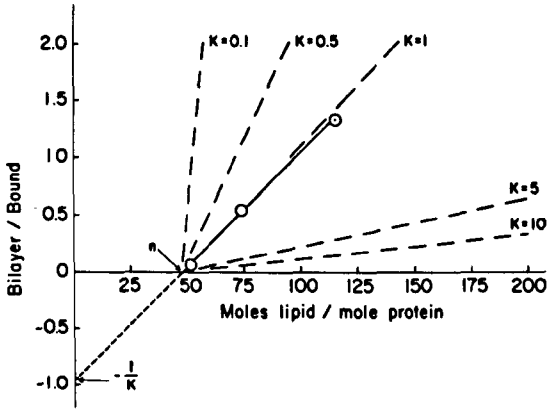

FIG. 10. A plot of Equation 5 derived from the multiple equilibrium site model for n=48 independent equivalent sites with relative binding constants ranging from 0.1 to 10. The circles are experimental values for cytochrome oxidase in its native lipids, labeled with 16-doxyl stearic acid at a label:protein ratio of 1:2. Reproduced from ref. [19].

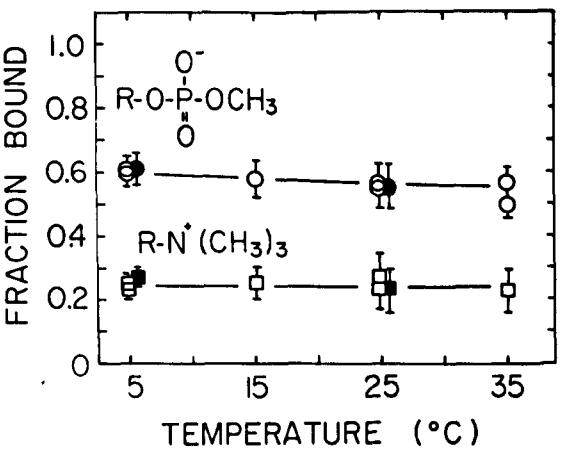

FIG. 11. The effect of head group charge and temperature on the equilibrium of lipid spin labels between the protein surface and the bilayer. The R group on the labels is 14-proxylstearic acid, and the sample is detergent-free (Na,K)-ATPase isolated with its native lipids from eel electric organ. The filled symbols indicate the use of single-component spectral subtraction. The open symbols use a pairwise subtraction method that makes no assumptions about the individual component line shapes [3]. Vertical lines indicate the range of systematic error introduced by deliberate over- and under-subtraction in both methods of data analysis. The neutral labels, not shown here, gave intermediate values for the fraction bound. At all temperatures the differences between the charged labels is reversibly abolished in the presence of 2 M LiCl. Modified from ref. [3].

Assuming one relative binding constant for L*, and assuming very low concentrations of label, a useful approximate solution of the equilibrium binding equation is

$$y = \frac{x}{nK} - \frac{1}{K} \qquad (15)$$

so that a plot of the lipid/protein ratio (x) versus the observed ratio of bilayer to bound (y) gives a straight line with a y-intercept of $-1/K$, x-intercept of n, and a slope of $1/nK$. As defined, K is the binding constant of the labeled lipid relative to the unlabeled lipid. The dashed lines of Fig. 10 show the theoretical lines expected for relative binding constants of 0.1 to 10 and demonstrate that this type of plot is sensitive to K. Also plotted are three experimental points for a fatty acid spin label equilibrated between the protein surface and the fluid bilayer. The approximate value of K=1 indicates that this label reflects the average behavior of the unlabeled lipids. The value of n indicates that a large number of lipids (about 45–50) are contacting the protein, and this number of contact sites roughly corresponds to the number of lipid chains that can be accommodated at the protein periphery. This does not rule out protein-protein contacts or the existence of a few high-affinity binding sites not accessible to this spin labeled lipid.

Recently, a modification of this general approach has been applied to a study of the (Na,K)-ATPase to investigate the role of charge in the equilibrium established between the bilayer and the boundary layer. The lipid labels used were identical except for the head group, so that any perturbation due to the reporter group is factored out. The membranous (Na,K)-ATPase purified from eel electric organ showed a definite preference for negatively-charged lipid (Fig. 11), even though the bilayer is a mixture of native lipids [3]. The fraction bound decreased from about 0.57 for a negatively charged label to about 0.25 for the positively-charged analog. In terms of the equilibrium binding constant formalism, the relative affinity is a function of the ratio of bound to bilayer components, and these ratios decrease from 1.3 to 0.33 when the negatively-charged lipid is compared to the positively charged. The neutral analogs, such as those with the dimethylphosphate or alcohol head groups, give an intermediate value of 0.54. The number of sites was not determined, but may well be only a fraction of the number of available contact sites. The charge preference persisted above physiological salt concentrations but was abolished at very high (2 M) salt. This indicates that the interaction is electrostatic. The charge selectivity of binding is similar to the trend in efficiency of various amphiphiles in the reactivation of this enzyme [34], also suggesting that some of the acidic lipids directly bind to the protein. Recently, it has been reported that the inhibitory action of ethanol on (Na,K)-ATPase activity (mouse brain) is related to the presence of the negatively-charged lipid phosphatidylserine, but is not affected by phosphatidylcholine, which has no net negative charge [37]. A preference for negatively charged lipid has also been observed in photosynthetic membranes of *Rhodopseudomonas sphaeroides* [2]. In both of these systems, the differences in relative binding detected by spin labeling are significant but not large enough to indicate highly selective binding. Thus, the lipids in the boundary layer as a whole do not constitute a specialized class of lipid. The selectivity seen might involve only a few sites, but these sites could be of considerable importance in the protein function.

In conclusion, all the spectroscopic data on membranes emphasize the dynamic nature of lipid-lipid and lipid-protein interactions. There is general qualitative agreement on the flexibility profile, anisotropic motion and lateral diffusion of both lipids and proteins. The studies of lipid-protein interactions have generated some controversy, but the picture emerging is one of a transient protein solvation layer that can be detected spectroscopically. This lipid exchanges with the adjacent bilayer. In some cases there is evidence that charged amino residues on the protein interact electrostatically with charges on the lipid headgroup, influencing the

time-averaged composition of the boundary layer. The role of this layer of lipid probably lies in preventing indiscriminate protein-protein aggregation (precipitation in the plane of the bilayer). In addition, a limited number of sites at the protein-lipid interface are the most probable region of any specific influence of lipid composition on protein function.

ACKNOWLEDGMENTS

We have profited from discussions on fluorescence techniques with Dr. Bruce Hudson who also supplied us Fig. 4 in advance of publication. Debra McMillen and Douglas Habliston provided us with valuable assistance in the preparation of this manuscript. We acknowledge general support from the National Institutes of Health, GM 25698-13.

REFERENCES

1. Axelrod, D., D. E. Koppel, J. Schlesinger, E. Elson and W. W. Webb. Mobility measurement by analysis of photobleaching recovery kinetics. *Biophys. J.* **16**: 1055–1069, 1976.
2. Birrell, G. B., W. R. Sistrom and O. H. Griffith. Lipid-protein associations in chromatophores from the photosynthetic bacterium *Rhodopseudomonas sphaeroides*. *Biochemistry* **17**: 3768–3773, 1978.
3. Brotherus, J. R., P. C. Jost, O. H. Griffith, J. F. W. Keana and L. E. Hokin. Charge selectivity at the lipid-protein interface of membranous Na,K-ATPase. *Proc. natn. Acad. Sci. U.S.A.* **77**: 272–276, 1980.
4. Cantor, C. R. and P. R. Schimmel. *Biophysical Chemistry, Part II. Techniques for the Study of Biological Structure and Function*. San Francisco: W. H. Freeman and Company, 1980, pp. 433–465.
5. Carrington, A. and A. D. McLachlan. *Introduction to Magnetic Resonance*. New York: Harper and Row Publishers, 1967, pp. 259–260.
6. Cherry, R. J. Rotational and lateral diffusion of membrane proteins. *Biochim. Biophys. Acta* **559**: 289–327, 1979.
7. Cone, R. A. Rotational diffusion of rhodopsin in the visual receptor membrane. *Nature, Lond.* **236**: 39–43, 1972.
8. Davis, J. H., M. Bloom, K. W. Butler and I. C. P. Smith. *Acholeplasma laidlawii* membranes: temperature dependence of molecular order and the influence of cholesterol. *Biochim. Biophys. Acta* **597**: 477–491, 1980.
9. Devaux, P. and H. M. McConnell. Lateral diffusion in spin-labeled phosphatidylcholine multilayers. *J. Am. Chem. Soc.* **94**: 4475–4481, 1972.
10. Edidin, M. Rotational and translational diffusion in membranes. *Ann. Rev. Biophys. Bioengineering* **3**: 179–201, 1974.
11. Elson, E. L., J. Schlessinger, D. E. Koppel, D. Axelrod and W. W. Webb. Measurement of lateral transport on cell surfaces. In: *Membranes and Neoplasia: New Approaches and Strategies*. New York: Alan R. Liss, Inc., 1976, pp. 137–147.
12. Engelman, D. M., R. Henderson, A. D. McLachlan and B. A. Wallace. Path of the polypeptide in bacteriorhodopsin. *Proc. natn. Acad. Sci. U.S.A.* **77**: 2023–2027, 1980.
13. Freed, J. Theory of slow tumbling ESR spectra for nitroxides. In: *Spin Labeling; Theory and Applications, Vol. 1*, edited by L. J. Berliner. New York: Academic Press, 1976, pp. 53–131.
14. Frye, L. D. and M. Edidin. The rapid intermixing of cell surface antigens after formation of mouse-human heterokaryons. *J. Cell Sci.* **7**: 319–335, 1970.
15. Fuller, S. D., R. A. Capaldi and R. Henderson. Structure of cytochrome *c* oxidase in deoxycholate-derived two-dimensional crystals. *J. molec. Biol.* **134**: 305–327, 1979.
16. Gaber, B. P. and W. L. Peticolas. On the quantitative interpretation of biomembrane structure by Raman spectroscopy. *Biochim. Biophys. Acta* **465**: 260–274, 1977.
17. Gaffney, B. J. Practical considerations for the calculations of order parameters for fatty acid or phospholipid spin labels in membranes. In: *Spin Labeling, Theory and Applications, Vol. 1*, edited by L. J. Berliner. New York: Academic Press, 1976, pp. 567–571.
18. Griffith, O. H. and P. C. Jost. Lipid spin labels in biological membranes. In: *Spin Labeling; Theory and Applications, Vol. 1*, edited by L. J. Berliner. New York: Academic Press, 1976, pp. 453–523.
19. Griffith, O. H. and P. C. Jost. The lipid-protein interface in cytochrome oxidase. In: *Cytochrome Oxidase*, edited by B. Chance, T. E. King, K. Okunuki and Y. Orii. Amsterdam: Elsevier/North Holland Biomedical Press, 1979, pp. 207–218.
20. Haughland, R. P. and L. Stryer. A fluorescent probe at the active site of α-chymotrypsin. In: *Conformation of Biopolymers, Vol. 1*, edited by G. N. Ramachandran. New York: Academic Press, 1967, pp. 321–335.
21. Heyn, M. P. Determination of lipid order parameters and rotational correlation times from fluorescence depolarization experiments. *FEBS Lett.* **108**: 359–364, 1979.
22. Henderson, R. and P. N. T. Unwin. Three-dimensional model of purple membrane obtained by electron microscopy. *Nature* **257**: 28–32, 1975.
23. Hirata, F. and J. Axelrod. Enzymatic synthesis and rapid translocation of phosphatidylcholine by two methyltransferases in erythrocyte membranes. *Proc. natn. Acad. Sci. U.S.A.* **75**: 2348–2352, 1978.
24. Hirata, F., W. J. Strittmatter and J. Axelrod. β-Adrenergic receptor agonists increase phospholipid methylation, membrane fluidity, and β-adrenergic receptor-adenylate cyclase coupling. *Proc. natn. Acad. Sci. U.S.A.* **76**: 368–372, 1979.
25. Hubbell, W. L. and H. M. McConnell. Molecular motion in spin-labeled phospholipids and membranes. *J. Am. Chem. Soc.* **93**: 314–326, 1971.
26. Hyde, J. S. Saturation-transfer spectroscopy. In: *Methods of Enzymology, Vol. XLIX, Enzyme Structure, Part G*, edited by C. H. W. Hirs and S. N. Timasheff. New York: Academic Press, 1978, pp. 480–511.
27. Jost, P., L. J. Libertini, V. C. Hebert and O. H. Griffith. Lipid spin labels in lecithin multilayers. A study of motion along fatty acid chains. *J. Molec. Biol.* **59**: 77–98, 1971.
28. Jost, P. C., A. S. Waggoner and O. H. Griffith. Spin labeling and membrane structure. In: *Structure and Function of Biological Membranes*, edited by L. Rothfield. New York: Academic Press, 1971, pp. 83–144.
29. Jost, P. C., O. H. Griffith, R. A. Capaldi and G. Vanderkooi. Evidence for boundary lipid in membranes. *Proc. natn. Acad. Sci. U.S.A.* **70**: 480–484, 1973.
30. Jost, P. C. and O. H. Griffith. Lipid-protein interactions: Influence of integral membrane proteins on bilayer lipids. In: *Biomolecular Structure and Function*, edited by P. F. Agris. New York: Academic Press, 1977, pp. 25–54.
31. Jost, P. C., K. K. Nadakavukaren and O. H. Griffith. Phosphatidylcholine exchanges between the boundary lipid and bilayer domains in cytochrome oxidase containing membranes. *Biochemistry* **16**: 3110–3114, 1977.
32. Jost, P. C. and O. H. Griffith. The spin labeling technique. In: *Methods of Enzymology, Vol. XLIX, Enzyme Structure, Part G*, edited by C. H. W. Hirs and S. N. Timsheff. New York: Academic Press, 1978, pp. 369–418.
33. Kawato, S., K. Kinosita and A. Ikagami. Effect of cholesterol on the molecular motion in the hydrocarbon region of lecithin bilayers studied by nanosecond fluorescence techniques. *Biochemistry* **17**: 5026–5031, 1978.
34. Kimelberg, H. K. Protein-liposome interactions and their relevance to the structure and function of cell membranes. *Molec. Cell. Biochem.* **10**: 171–190, 1976.
35. Knowles, P. F., A. Watts and D. Marsh. Lipid immobilization in dimyristoylphosphatidylcholine-substituted cytochrome oxidase. *Biochemistry* **18**: 4480–4487, 1979.

36. Koppel, D. E., D. Axelrod, J. Schlessinger, E. L. Elson and W. W. Webb. Dynamics of fluorescence marker concentration as a probe of mobility. *Biophys. J.* **16**: 1315–1329, 1976.
37. Lin, D. C. Involvement of the lipid and protein components of the (Na^+ and K^+)-adenosine triphosphatase in the inhibitory action of alcohol. *Biochem. Pharmac.* **29**: 771–775, 1980.
38. McConnell, H. M. Molecular motion in biological membranes. In: *Spin Labeling, Theory and Applications, Vol. 1*, edited by L. J. Berliner. New York: Academic Press, 1976, pp. 525–560.
39. McConnell, H. M. and B. G. McFarland. The flexibility gradient in biological membranes. *Ann. N.Y. Acad. Sci.* **195**: 207–217, 1972.
40. Oldfield, E., R. Gilmore, M. Glaser, H. S. Gutowsky, J. C. Hsung, S. Y. Kang, T. E. King, M. Meadows and D. Rice. Deuterium nuclear magnetic resonance investigation of the effects of proteins and polypeptides on hydrocarbon chain order in model membrane systems. *Proc. natn. Acad. Sci. U.S.A.* **75**: 4657–4660, 1978.
41. Rothman, J. E. and J. Lenard. Membrane asymmetry. *Science* **195**: 743–753, 1977.
42. Seelig, J. Anisotropic motion in liquid crystalline structures. In: *Spin Labeling, Theory and Applications, Vol. 1*, edited by L. J. Berliner. New York: Academic Press, 1976, pp. 373–409.
43. Seelig, J. Deuterium magnetic resonance: theory and application to lipid membranes. *Q. Rev. Biophys.* **10**: 353–418, 1977.
44. Seelig, J. and A. Seelig. The dynamic structure of fatty acyl chains in a phospholipid bilayer measured by deuterium magnetic resonance. *Biochemistry* **13**: 4839–4845, 1974.
45. Seelig, A. and J. Seelig. Lipid-protein interactions in reconstituted cytochrome c model membranes. *Hoppe-Seyler's Z. Physiol. Chem.* **359**: 1747–1756, 1978.
46. Shinitsky, M. and M. Inbar. Differences in microviscosity induced by different cholesterol levels in the surface membrane lipid layer of normal lymphocytes and malignant lymphoma cells. *J. molec. Biol.* **85**: 603–615, 1974.
47. Singer, S. J. The molecular organization of membranes. In: *Structure and Function of Membranes*, edited by L. I. Rothfield. New York: Academic Press, 1971, pp. 146–222.
48. Singer, S. J. and G. L. Nicolson. The fluid mosaic model of the structure of cell membranes. *Science* **175**: 720–731, 1972.
49. Smith, B. A. and H. M. McConnell. Determination of molecular motion in membranes using periodic pattern photobleaching. *Proc. natn. Acad. Sci. U.S.A.* **75**: 2759–2763, 1978.
50. Taylor, R. B., P. H. Duffus, M. C. Raff and S. de Petris. Redistribution and pinocytosis of lymphocyte surface immunoglobulin molecules induced by anti-immunoglobulin antibody. *Nature New Biol.* **233**: 225–229, 1971.
51. Stryer, L. Fluorescence spectroscopy of proteins. *Science* **162**: 526–533, 1968.
52. Thompson, T. E. Transmembrane compositional asymmetry of lipids in bilayers and biomembranes. In: *Molecular Specialization and Symmetry in Membrane Function*, edited by A. K. Solomon and M. Karnovsky. Cambridge, MA: Harvard University Press, 1978, pp. 79–98.
53. Träuble, H. and E. Sackman. Studies of the crystalline-liquid phase transition of lipid model systems. III. Structure of a steroid-lecithin system below and above the lipid-phase transitions. *J. Am. Chem. Soc.* **94**: 4499–4510, 1972.
54. Unwin, P. N. T. and R. Henderson. Molcular structure determination by electron microscopy of unstained crystalline specimens. *J. molec. Biol.* **94**: 425–440, 1975.
55. Veatch, W. R. and L. Stryer. Effect of cholesterol on the rotational mobility of diphenylhexatriene in liposomes: a nanosecond fluorescence anisotropy study. *J. molec. Biol.* **117**: 1109–1113, 1977.
56. Watts, A., I. D. Volotovski and D. Marsh. Rhodopsin-lipid associations in bovine rod outer segment membranes. Identification of immobilized lipid by spin-labels. *Biochemistry* **18**: 5006–5013, 1979.